Transition States for Hydroalumination of Alkenes and Alkynes: Ab Initio Molecular Orbital Studies

Jeanne Wilson Bundens and Michelle Miller Francl*

Department of Chemistry, Bryn Mawr College, 101 North Merion Avenue, Bryn Mawr, Pennsylvania 19010-2899

Received October 22, 1992

The insertion reaction of an alkene or alkyne into an Al–H bond as well as its reverse reaction, β-hydride elimination, were investigated. High level ab initio molecular orbital techniques were used to characterize the transition structure which connects the intermediate π-complex of the aluminum alkyl and the alkene or alkyne to the insertion product. An analysis of the bonding and relative energies of various methyl-substituted transition structures provides insight into the factors controlling the regio- and stereochemistry of the final products.

In the hands of an organic synthetic chemist, the broad classes of addition and elimination reactions become fundamental construction tools. Reactions by which the size or complexity of the carbon skeleton may be altered are particularly attractive additions to the repertoire. Alkylaluminum complexes rank among the more commonly employed agents for carbon–carbon and carbon–hydrogen bond formation.[1] For example, the insertion of an alkene or alkyne into the Al–H bond of an alkyl aluminum hydride is a key first step in the route to the formation of a new carbon–hydrogen bond via hydroalumination. Such an insertion process is also part of the oligomerization of α-olefins catalyzed by alkylaluminum hydrides, i.e. the Ziegler process. The reverse of this step, β-hydride elimination of an alkyl ligand from a trialkylaluminum complex, is important in understanding aluminum chemical vapor deposition, a step in the manufacturing process for integrated circuits. In order to further our understanding of the underlying factors which affect this fundamental reaction motif, we have used ab initio molecular orbital methods to probe the reaction path for the insertion of carbon–carbon multiple bonds into Al–H bonds.

During the past decade several theoretical studies of the hydroalumination of ethylene and acetylene have appeared. These have consistently suggested that the reaction involves a symmetric π-complex intermediate linked to the insertion product by a four-centered (Al, H*,[2] C, C) transition state as shown in Figure 1. Experimental work by Egger supports these results.[3] The alternative π-complex transition state proposed by Eisch,[4] however, is inconsistent with both the theoretical studies and the experimental work of Egger and others. In 1981 Gropen and Haaland characterized the transition structure for the insertion of acetylene into the Al–H bond of alane.[5] One year later, they reported the transition structure for the analogous insertion reaction of AlH_3 with ethylene.[6] Okninski and Starowieyski in 1986 used a semiempirical localized molecular orbital approach to examine the

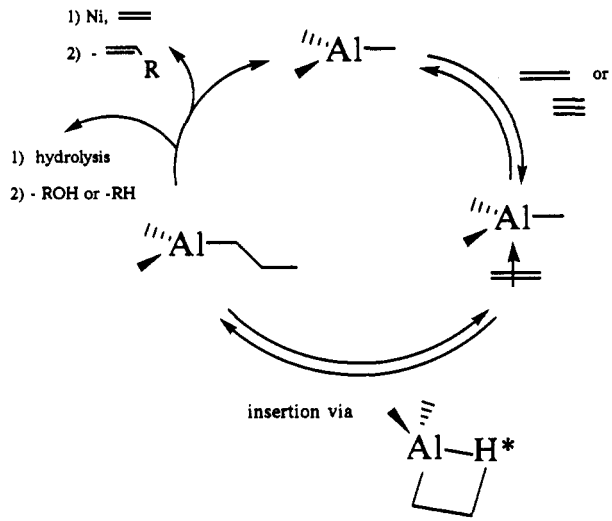

Figure 1. Proposed scheme connecting π-complex intermediates and insertion products resulting from addition of alkylaluminum complexes to alkenes and alkynes.

question of whether the four-centered transition structure was symmetry forbidden.[7] On the basis of their theoretical study of electron migration over the course of the reaction, they concluded the reaction of AlH_3 with acetylene was nonsynchronous. Recently, Sakai described a similar push–pull two-stage mechanism for the analogous reaction of AlH_3 with ethylene.[8] Sakai's charge analysis suggested that the initial Al–C bond formation occurs more rapidly than the breaking of Al–H* and the making of C–H* bonds. The reverse reaction was studied by Higashi et al. in the context of its application to chemical vapor deposition.[9] They examined the four-centered AlH_3 + ethylene transition structure using more sophisticated theoretical models than those used previously, though no substantial differences were found.

Houk et al.[10] and others[11] have examined the reaction

(1) Larock, R. C. *Comprehensive Organic Transformations*; VCH Publishers, Inc.: New York, 1989; pp 223–226.
(2) H* designates the H which is being transferred from the Al to the substrate alkyne or alkene.
(3) Egger, K. W. *J. Am. Chem. Soc.* **1969**, *91*, 2867.
(4) Eisch, J. J. *Comprehensive Organometallic Chemistry*; Wilkinson, G., Stone, F. G. A., Abel, E. W., Eds.; Pergamon: Oxford, U.K., 1982; Chapter 6.
(5) Gropen, O.; Haaland, A. *Acta Chem. Scand., Ser. A* **1981**, *35*, 305.
(6) Gropen, O.; Haaland, A. *Acta Chem. Scand., Ser. A* **1982**, *36*, 435.
(7) Okninski, A.; Starowieyski, K. B. *J. Mol. Struct. (THEOCHEM)* **1986**, *138*, 249.
(8) Sakai, S. *J. Phys. Chem.* **1991**, *95*, 175.
(9) Higashi, G. S.; Raghavachari, K.; Steigerwald, M. L. *J. Vac. Sci. Technol., B* **1990**, *8*, 103.
(10) (a) Houk, K. N.; Rondan, N. G.; Wu, Y-D.; Metz, J. T.; Paddon-Row, M. N. *Tetrahedron* **1984**, *40*, 2257. (b) Wang, X.; Li, Y.; Wu, Y-D.; Paddon-Row, M. N.; Rondan, N. G.; Houk, K. N. *J. Org. Chem.* **1990**, *55*, 2601.
(11) Nagase, S.; Ray, N. K.; Morokuma, K. *J. Am. Chem. Soc.* **1980**, *102*, 4536.

0276-7333/93/2312-1608$04.00/0

Table I. Comparison of Optimized Transition-State Core Parameters for Various Basis Sets[a]

TS	basis set	θ, deg	ϕ, deg	Al–H*, Å	Al–C_α, Å	C–C, Å
$AlH_3 + C_2H_4$	3-21G(*)	79.8	83.6	1.691	2.136	1.405
	6-31G*	79.6	83.1	1.690	2.135	1.402
	6-31G**	79.3	83.3	1.685	2.140	1.400
	6-311+G*	79.4	83.2	1.682	2.136	1.401
	MP2/6-311+G*	76.1	85.8	1.668	2.154	1.402
$AlH_3 + C_2H_2$	3-21G(*)	84.2	82.2	1.675	2.132	1.241
	6-31G*	83.8	82.4	1.669	2.124	1.234
	6-311+G*	83.6	82.5	1.664	2.124	1.234
AlH_3 + propene	3-21G(*)	81.2	83.3	1.687	2.116	1.413
	6-31G*	81.4	82.7	1.688	2.113	1.413
AlH_3 + propyne	3-21G(*)	86.6	81.4	1.676	2.098	1.248
	6-31G*	86.7	81.8	1.671	2.090	1.246
	6-311+G*	86.6	81.8	1.666	2.090	1.243

[a] Parameter labels are as shown below.

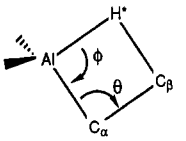

path for the analogous hydroboration reaction with a variety of substrates. The intermediates and transition structures found in these studies are consistent with those for the hydroalumination pathway described in Figure 1. Qualitatively, the energetics of these pathways compare well with those from the simple hydroalumination reactions studied heretofore. Schleyer and Hommes[12] have examined the structure of the transition structure for the reaction of dimethylboron and ethylene using correlated methods and suggest that it is a three-centered rather than four-centered structure.

Our group has previously characterized the π-complex intermediates for hydroalumination.[13] The present work examines the transition structures connecting these intermediates with their insertion products. The reaction archetypes of AlH_3 with ethylene and acetylene are explored using ab initio molecular orbital theory and post-Hartree–Fock methods. In addition, the transition structures for AlH_3 with propene and propyne as well as other methyl-substituted variations on the archetypical transition structures are presented along with their related intermediates and products.

Methods

Ab initio molecular orbital calculations were performed to characterize the reaction pathways using the GAUSSIAN 8X suite of programs[14] and SPARTAN.[15] Optimized structures were initially determined at the HF/3-21G(*)[16] level. Transition structures were identified as critical points having one and only one imaginary normal mode vibrational frequency, while stable structures were confirmed to have no imaginary frequencies. Selected structures were optimized at the post-Hartree–Fock level using larger basis sets.

Reaction energies and barriers were determined using post-Hartree–Fock methods for the archetypical reactions and using the HF/3-21G(*) results for other systems (vide infra for a discussion of the validity of this procedure). Single-point energy calculations using the 3-21G(*)-optimized geometry were done at the MP2, MP3, and MP4/6-311+G**[17,18] levels. Where indicated, corrections were made for zero-point vibrational energies and to temperatures representative of those used in experimental work.[19]

The standard 3-21G(*) basis set was employed for most of the initial geometry optimizations as previous studies have shown it to be adequate to establish the optimized geometries of the intermediate π-complexes and their related reactants and products.[13,20] We find in the present study that HF/3-21G(*) descriptions of the geometries of transition states are comparable to those extracted from higher level calculations. Benchmark optimizations of four transition structures using the larger bases 6-31G*[21] and 6-311+G* changed the bond-breaking and bond-making

(12) Hommes, N. J. R. v. E.; Schleyer, P. v. R. *J. Org. Chem.* **1991**, *56*, 4074.

(13) Chey, C.; Choe, H.-S.; Chook, Y.-M.; Jensen, E.; Seida, P. R.; Francl, M. M. *Organometallics* **1990**, *9*, 2430.

(14) Binkley, J. S.; Frisch, M.; Krishnan, R.; Defrees, D. J.; Schlegel, H. B.; Whiteside, R.; Fluder, E.; Seeger, R.; Pople, J. A. *GAUSSIAN 82*; Carnegie-Mellon University: Pittsburgh, PA, 1982. Frisch, M. J.; Head-Gordon, M.; Schlegel, H. B.; Raghavachari, K.; Binkley, J. S.; Gonzalez, C.; Defrees, D. J.; Fox, D. J.; Whiteside, R. A.; Seeger, R.; Melius, C. F.; Baker, J.; Martin, R. L.; Kahn, L. R.; Stewart, J. J. P.; Fluder, E. M.; Topiol, S. and Pople, J. A. *GAUSSIAN 88*; Gaussian, Inc., Pittsburgh, PA.

(15) *SPARTAN*; Wavefunction, Inc.: Irvine, CA.

(16) (a) First-row elements: Binkley, J. S.; Pople, J. A.; Hehre, W. J. *J. Am. Chem. Soc.* **1980**, *102*, 939. (b) Second-row elements: Pietro, W. J.; Francl, M. M.; Hehre, W. J.; Defrees, D. J.; Pople, J. A.; Binkley, J. S. *J. Am. Chem. Soc.* **1982**, *104*, 5039. The basis set includes polarization functions on second-row elements only. The supplemental functions provide added flexibility for the descriptions of molecules in which the valence octet has been formally exceeded, a common occurrence for compounds containing second-row elements. These functions are not considered part of the formal valence shell, and are thus not split.

(17) Moller, C.; Plesset, M. S. *Phys. Rev.* **1934**, *46*, 618. Binkley, J. S.; Pople, J. A. *Int. J. Quantum Chem.* **1975**, *9*, 229. Binkley, J. S.; Pople, J. A.; Seeger, R. *Int. J. Quantum Chem.* **1976**, *S10*, 1. Krishnan, R.; Pople, J. A. *Int. J. Quantum Chem.* **1978**, *14*, 91. Krishnan, R.; Frisch, M. J.; Pople, J. A. *J. Chem. Phys.* **1980**, *72*, 4244.

(18) Krishnan, R.; Frisch, M. J.; Pople, J. A. *J. Chem. Phys.* **1980**, *72*, 650. Frisch, M. J.; Binkley, J. S.; Pople, J. A. *J. Chem. Phys.* **1984**, *80*, 3265. The 6-311+G** basis includes both diffuse and polarization functions on heavy atoms and p-type polarization functions on hydrogen.

(19) Correction for zero-point vibrational energy:

$$H_{vib}(0) = {}^1/_2 h \sum_i^{\text{normal modes}} \nu_i$$

Correction to T = 298 K:

$$\Delta H(T) = H_{trans}(T) + H_{rot}(T) + \Delta H_{vib}(T) + RT$$

$$H_{trans}(T) = {}^3/_2 RT$$

$$H_{rot}(T) = {}^3/_2 RT \text{ (If linear, } RT\text{)}$$

$$\Delta H_{vib}(T) = Nh \sum_i^{\text{normal modes}} \nu_i / (e^{h\nu_i/kT} - 1)$$

Where each frequency, ν_i, was calculated at 3-21G(*) and scaled by 0.9. If $\nu_i < 500$ cm^{-1}, then it was counted as ${}^1/_2 RT$; imaginary frequencies for transition states were not included in the treatment.

(20) Hehre, W. J.; Radom, L.; Schleyer, P. v. R.; Pople, J. A. *Ab Initio Molecular Orbital Theory*; Wiley, New York, 1986.

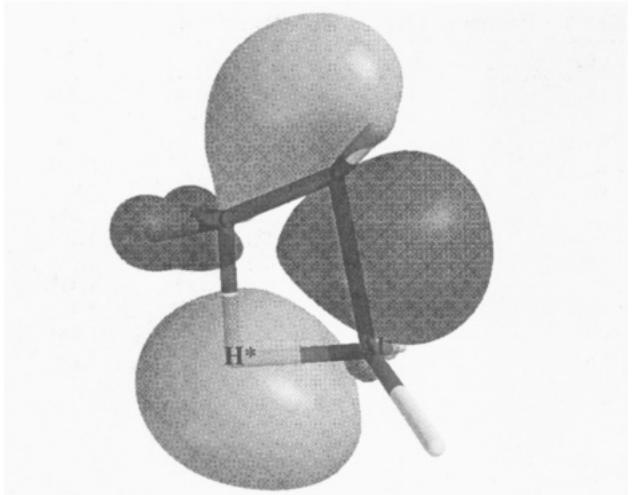

Figure 2. Molecular orbital plot of the transition state for the addition of ethylene to AlH_3 showing the degradation of the C–C π-system concomitant with the formation of the C–H* bond. The asterisk indicates the H that is being transferred.

parameters by at most 0.01 Å for bond lengths and by less than 0.7° for bond angles (refer to Table I). Addition of polarization functions to the hydrogen basis (6-31G**) for the optimization of the transition state for the addition of ethylene to AlH_3 also did not affect the bond-making/breaking parameters. Optimizing the AlH_3 + ethylene transition structure at the more computationally demanding MP2/6-311+G* level changed these parameters by no more than 0.02 Å and less than 4°. Optimizations of the BH_3 with the ethylene transition structure at 3-21G and MP2/3-21G also showed little difference in parameter values (0.02 Å and less).[10b] However, Hommes and Schleyer[12] found electron correlation to be important in the geometry optimization of dimethylboron hydride with ethylene: C–H* distances at MP2/6-31G* and MP2/6-31G** were found to be 0.25 and 0.33 Å longer than at HF/6-31G*. We do not see such dramatic changes in the corresponding aluminum transition structures as electron correlation is included. For example, the change in the C–H* bond length is only 0.02 Å between the HF/6-31G* and MP2/6-311+G* levels. The HF/3-21G(*) level appears to be sufficient to the task of computing the geometries of the transition structures for these organoaluminum systems.

Atomic charges were determined by fitting point charges centered on the atoms to the molecular electrostatic potential function. A modified version of CHELP[22] was used. Between 20 000 and 40 000 total points were used for each fit, chosen to be outside the van der Waals envelope of each molecule.[23] The average root mean square (rms) deviation of the electrostatic potential from the monopole fit was generally less than 10 kcal mol^{-1}. Increasing the number of points led to a reduction in the rms deviation without significantly affecting the charges.

(21) (a) First-row elements: Hahrihan, P. C.; Pople, J. A. *Theor. Chim. Acta* **1973**, *28*, 213. (b) Second-row elements: Francl, M. M.; Pietro, W. J.; Hehre, W. J.; Binkley, J. S.; Defrees, D. J.; Pople, J. A.; Gordon, M. S. *J. Chem. Phys.* **1982**, *77*, 3654.

(22) CHELP: Chirlian, L. E.; Francl, M. M. *J. Comput. Chem.* **1987**, *8*, 894; Chirlian, L. E.; Francl, M. M. *QCPE* **1987**, *7*, 39. CHELP II: Chirlian, L. E.; Francl, M. M. to be submitted to the Quantum Chemistry Program Exchange.

(23) van der Waals atomic radii in angstroms used in determining the molecular van der Waals surface: Al, 2.5; C, 1.8; H, 1.2. Values for C and H were reported: Francl, M. M.; Hout, R. F., Jr.; Hehre, W. J. *J. Am. Chem. Soc.* **1984**, *106*, 563. Aluminum radius determined by best fit to HF/3-21G(*) electron density surface.

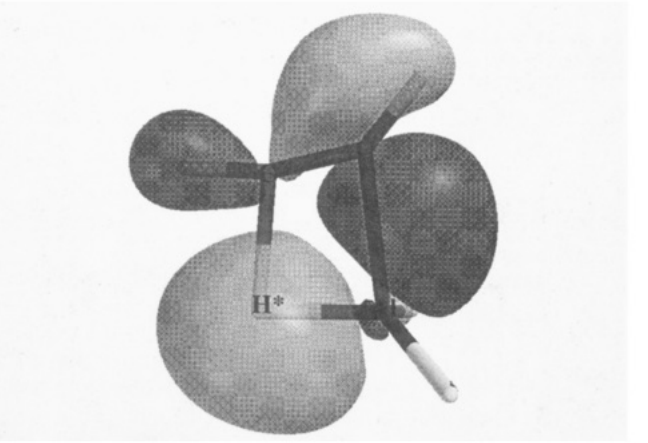

Figure 3. Molecular orbital plot of the transition state for the addition of acetylene to AlH_3 showing the degradation of the in-plane C–C π-system concomitant with the formation of the C–H* bond. The asterisk indicates the H that is being transferred.

Results and Discussion

A. Bonding in the Transition Structures. While the carbon–carbon bond lengths are not significantly affected by binding to the aluminum in the π-complex intermediates, we see significant lengthening in the transition structures as the π-systems delocalize into the forming Al–C and C–H* [2] bond regions. This can be clearly seen by examining the molecular orbitals for the transition structure of ethylene inserting into the Al–H bond of alane. The MO plot in Figure 2 shows the degradation of the C–C π-system accompanied by the formation of the C–H* bond. Typical C–C distances for the alkene-based intermediates are 1.327–1.338 Å, within the range for normal C–C double bonds.[24] By comparison, those in the transition structure average 6% longer, ranging from 1.403 to 1.422 Å. The MO plot of the analogous AlH_3 + acetylene transition structure in Figure 3 conveys a similar picture of the transformation process including the forming Al–C bond in the HOMO of the system. The range of C–C distances for the acetylene-based intermediates is 1.192–1.196 Å. Again, these values are within the normal range for C–C triple bonds, a finding concomitant with their weak binding energies. The C–C bond in the corresponding transition structures lengthens by approximately 4% to give a range of 1.240–1.250 Å, still about 0.1 Å shorter than the final C–C double bond of the insertion product.

Calculations on the π-intermediates suggest that substantial charge-transfer has taken place between the AlR_3 fragment and the complexed alkene or alkyne.[25] The corresponding transition structures exhibit much less charge-transfer. Atomic charge calculations show that total electron "transfer" between the aluminum fragment and the organic moiety is on the order of $0.10e^-$. Molecular orbital plots (Figures 2, 3 and 4) also confirm the covalent nature of the transition structures. Charges on the hydrogen undergoing transfer to the target organic fragment are, as expected, negative and support the typical description of these reactions as hydride transfer reactions.

Tables II–IV contain the critical bond-breaking and bond-making parameters for AlH_3 + ethylene and acet-

(24) Pople, J. A.; Gordon, M. S. *J. Am. Chem. Soc.* **1967**, *89*, 4253.

(25) Hommes, N. J. R. v. E.; Francl, M. M., unpublished calculations on $AlH_3C_2H_4$ complex. In addition, examination of the electron density surfaces and molecular electrostatic potentials in SPARTAN for a variety of π-intermediates are also strongly suggestive of significant charge transfer.

Table II. Selected Parameters for Intermediates Optimized at HF/3-21G(*)[a]

intermediate	Al–C_α (Å)	Al–C_β (Å)	C–C (Å)	C–Me or Al–Me (Å)	∠Al$C_\alpha C_\beta$ (deg)	∠Al$C_\beta C_\alpha$ (deg)	∠C_αCC (deg)
$AlH_3 + C_2H_4$	2.700		1.328		75.6		
$AlH_3 + C_2H_2$	2.726		1.193		79.3		
AlH_3 + propene	2.596	2.746	1.332	1.508	81.9	69.4	124.8
AlH_3 + propyne	2.706	2.640	1.196	1.468	74.0	80.2	177.9
$AlMeH_2 + C_2H_4$	2.761		1.327	1.984	76.0		
$AlMeH_2 + C_2H_2$	2.812		1.192	1.979	77.9		
AlH_3 + isobutene	2.467	2.924	1.338	1.515	95.8	57.1	121.6
AlH_3 + 2-butyne	2.606	2.673	1.198	1.473	80.0	73.8	175.3

[a] Bond lengths in angstroms and angles in degrees.

Table III. Selected Parameters for Transition States Optimized at HF/3-21G(*)[a]

reaction	Al–H*	Al–C_α	C_α–C_β	C_β–H*	C_α–Me or Al–Me	θ	ϕ
$AlH_3 + C_2H_4$	1.691	2.136	1.405	1.725		79.8	83.6
$AlH_3 + C_2H_2$	1.675	2.132	1.241	1.827		84.2	82.2
AlH_3 + propene	1.687	2.116	1.413	1.726		81.2	83.3
AlH_3 + propene[b]	1.694	2.127	1.410	1.710	1.533	79.4	83.7
AlH_3 + propyne	1.676	2.098	1.248	1.820		86.6	81.4
AlH_3 + propyne[b]	1.673	2.118	1.244	1.793	1.496	83.1	82.3
$AlMeH_2 + C_2H_4$	1.696	2.144	1.403	1.726	1.982	79.9	83.3
$AlMeH_2 + C_2H_2$	1.671	2.143	1.240	1.829	1.981	84.1	81.9
AlH_3 + isobutene	1.682	2.104	1.422	1.729		82.4	82.9
AlH_3 + 2-butyne	1.675	2.090	1.250	1.797	1.501	85.5	81.7
AlH_3 + *cis*-2-butene	1.690	2.109	1.422	1.709	1.533	80.8	83.4
$AlMeH_2$ + propene	1.692	2.125	1.411	1.728	1.984	81.3	82.9
$AlMe_2H + C_2H_4$	1.702	2.148	1.403	1.720	1.985	80.0	82.9

[a] Bond lengths in angstroms and angles in degrees. [b] Transition structure leading to Markovnikov addition product.

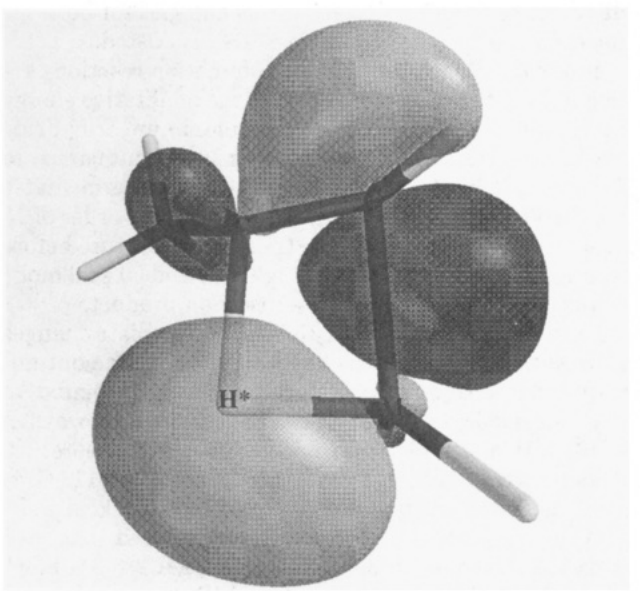

Figure 4. Molecular orbital plot of the transition state for the addition of propene to AlH_3 showing the degradation of the C–C π-system and formation of the C–H* bond. Note the overlap involving the staggered methyl group (see the text). The asterisk indicates the H that is being transferred.

Table IV. Selected Parameters for Products Optimized at HF/3-21G(*)[a]

reaction	Al–C	C–C	C–Me	∠CCAl	∠CCC
$AlH_3 + C_2H_4$	1.977	1.556		115.4	
$AlH_3 + C_2H_2$	1.952	1.331		121.9	
AlH_3 + propene	1.978	1.554	1.542	115.8	112.2
AlH_3 + propyne	1.946	1.334	1.511	121.4	125.6

[a] Bond lengths in angstroms and angles in degrees.

ylene transition structures, intermediates and products, and several of their methyl-substituted derivatives at HF/3-21G(*). Consistent with the majority of the previous hydroboration work,[10] we find the transition structure to be best represented by a four-centered structure. We also find that the four-centered core parameters of the various substituted transition structures differ from their respective unsubstituted transition structures by less than 0.05 Å or 2.6°.

Substitution effects in the transition structures were explored by replacing H with a methyl group at the aluminum center, at the β-C and at the α-C of the alkene or alkyne. Methyl substitution at aluminum in alkene transition structures tends to decrease the C–C bond length 0.002 Å while increasing the Al–C distance by 0.008 Å, suggesting a slightly earlier transition structure. In contrast, a methyl substituent at the β-C has a more significant effect: lengthening the C–C bond by 0.008 Å and shortening the Al–C bond by 0.02 Å. With two methyls at the β-C, the perturbation in the C–C distance is substantially larger (0.02 Å), while the Al–C distance shortens by 0.03 Å. In general, we find that substitution at the β–C produces a slightly later transition structure than in the unsubstituted system. Similarly, a methyl at the α-C lengthens the C–C bond (0.005 Å) and shortens the Al–C length (only 0.009 Å), also indicating a slightly later transition structure. These substitution patterns are observed with alkyne substrates, though the change in core parameters from the archetype of AlH_3 with acetylene is somewhat less significant. Methyl substituents at both α- and β-C result in a tighter transition structure for alkenes and alkynes. For example, the Al–C and C–H* distances decrease by between 0.02 and 0.04 Å for AlH_3 with *cis*-2-butene and 2-butyne.

B. Orientation of the Organic Fragments in the Transition Structures. For the reaction of AlH_3 with propene, the preferred insertion transition state positions the aluminum fragment nearer to the terminal carbon as expected, leading to anti-Markovnikov addition. The transition state leading to a Markovnikov product was found to be 5.6 kcal mol^{-1} greater in energy. For propyne,

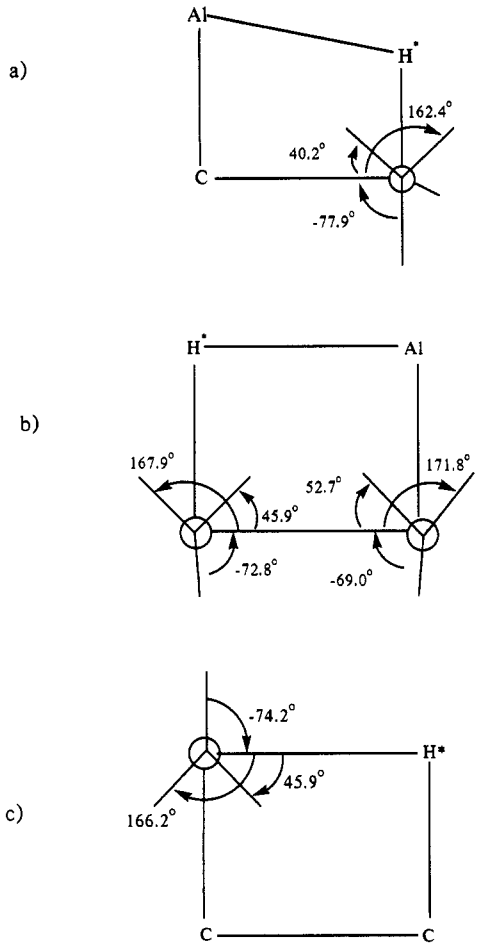

Figure 5. Newman projections showing preferred arrangement of methyl substituents in the transition structures for the reactions (a) $AlH_3 + C_3H_6$, (b) AlH_3 + *cis*-2-butene, and (c) $MeAlH_2 + C_2H_4$.

the difference in the two orientations is 3.5 kcal mol^{-1} and is also consistent with the anti-Markovnikov preference.

Houk's work on the hydroboration of methyl-substituted alkenes showed the preferred conformation of methyl substituents to be arranged such that the methyl C–H bonds are staggered with respect to forming and breaking bonds.[26] We find the analogous orientations are preferred for the hydroalumination reactions studied as well. The MO plot in Figure 4 shows delocalization over the π-system in the AlH_3 + propene transition structure including overlap with a staggered methyl C–H bond. See Figure 5 for the Newman projections of the AlH_3 + propene and *cis*-2-butene, and $MeAlH_3$ + ethylene transition structures with associated dihedral angles.

The weakly bound intermediate π-complexes show no significant preferences in orientation except for those expected from steric pressures.[13] The rotation about a pseudo C_3 axis connecting the AlH_3 fragment with the center of the ethylene double bond exhibits an apparent barrier of only 0.1 kcal mol^{-1} and with propene it is only 0.2 kcal mol^{-1}. Rotations of the ethylene insertion products around the Al–C bond are also facile, having barriers less than 0.5 kcal mol^{-1}. On the other hand, double bond-containing acetylene insertion products show some preference for aligning the C–C π-system with the empty

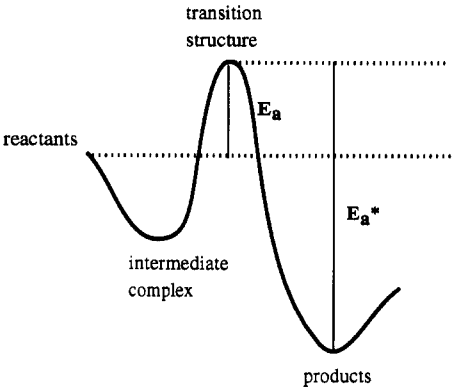

Figure 6. Qualitative energy profile for the hydroalumination reaction.

aluminum p orbital The Al–C bond rotational barrier is a more substantial 4 kcal mol^{-1} in the AlH_3 + acetylene insertion product. Presumably, this is due in part to the stabilization that can be achieved via delocalization of the π bond into the aluminum p orbital. In addition, such a structure would minimize the destabilizing secondary four electron interaction between an Al–H σ-bond and the C–C π-system.

C. Reaction Energies. Table V catalogues total energies for each transition structure, its corresponding reactants, and intermediate and insertion product for different basis sets. The activation energies for both the forward and backward reactions are also listed.

Forward Reaction. Hydroalumination reactions are understood to proceed as shown in the qualitative energy profile diagram in Figure 6. The aluminum trihydride and alkene or alkyne reactants collapse without barrier to form weakly bound π-complexes.[13] These intermediates are then thought to surmount a barrier on the order of 15 kcal mol^{-1} via a four-centered transition structure before forming the more stable (by roughly 35 and 50 kcal mol^{-1} respectively) alkene or alkyne insertion product.

Even though the geometry of the intermediate changes substantially as larger basis sets are used for the optimization, the energy of complexation for AlH_3 bound to ethylene remains remarkably constant[13] with no more than a 0.4 kcal mol^{-1} variation for the different theoretical models used. The highest level (MP4(SDTQ)/6-311+G**) gave calculated binding energies to AlH_3 of –9.6 kcal mol^{-1} for ethylene and –11.4 for propene, compared with –9.7 and –11.6 kcal mol^{-1}, respectively, at the MP2/6-311+G** level. For AlH_3 bound to acetylene, MP2/6-311+G** and the full MP4(SDTQ)/6-311+G** calculations both gave complexation energies of –8.3 kcal mol^{-1}.

The overall activation energy for conversion of reactants to transition structures is fairly low. Experimentally, Cocks and Egger estimate the barrier to addition of diethylaluminum hydride to ethylene to be about 4.9 kcal mol^{-1}.[27] Our highest level single point calculation at MP4(SDTQ)/6-311+G**//HF/3-21G(*) for the barrier to addition of ethylene to aluminum trihydride is of the same order of magnitude at 2.5 kcal mol^{-1}. A full optimization at MP2/6-311+G* results in a similar calculated barrier of 2.2 kcal mol^{-1}.

It is quite clear to us that inclusion of electron correlation and addition of diffuse functions to the basis is critical to the computation of absolute barriers, though full MP4

(26) (a) Paddon-Row, M. N.; Rondan, N. G.; Houk, K. N. *J. Am. Chem. Soc.* **1982**, *104*, 7162. (b) Houk, K. N.; Paddon-Row, M. N.; Rondan, N. G.; Wu, Y-D.; Brown, F. K.; Spellmeyer, D. C.; Metz, J. T.; Li, Y.; Longcharich, R. J. *Science* **1986**, *231*, 1108. See also ref 10a.

(27) Cocks, A. T.; Egger, K. W. *J. Chem. Soc., Faraday Trans. 1* **1972**, *68*, 423.

Table V. Total and Relative Energies for Reactants, Products, and Transition Structures at Various Theoretical Levels

reaction	structure	theoretical level	total energy (hartrees)	relative energy (kcal/mol)
$AlH_3 + C_2H_4$	reactants	HF/3-21G(*)//HF/3-21G(*)	−319.944 724	0.0
		MP2/6-311+G**//HF/3-21G(*)	−322.062 183	
		MP2/6-311+G*//MP2/6-311+G*	−322.167 566	
		MP3/6-311+G**//HF/3-21G(*)	−322.102 628	
		MP4/6-311+G**//HF/3-21G(*)	−322.121 874	
	π-complex	HF/3-21G(*)//HF/3-21G(*)	−319.960 313	−9.8
		MP2/6-311+G**//HF/3-21G(*)	−322.077 652	−9.7
		MP3/6-311+G**//HF/3-21G(*)	−322.117 669	−9.4
		MP4/6-311+G**//HF/3-21G(*)	−322.137 124	−9.6
	TS	HF/3-21G(*)//HF/3-21G(*)	−319.928 729	+10.0
		MP2/6-311+G**//HF/3-21G(*)	−322.058 156	+2.5
		MP2/6-311+G*//MP2/6-311+G*	−322.164 045	+2.2
		MP3/6-311+G**//HF/3-21G(*)	−322.096 501	+3.8
		MP4/6-311+G**//HF/3-21G(*)	−322.117 960	+2.5
	product	HF/3-21G(*)//HF/3-21G(*)	−319.995 541	−31.9
		MP2/6-311+G**//HF/3-21G(*)	−322.115 658	−33.6
		MP3/6-311+G**//HF/3-21G(*)	−322.154 722	−32.7
		MP4/6-311+G**//HF/3-21G(*)	−322.172 565	−31.8
$AlH_3 + C_2H_2$	reactants	HF/3-21G(*)//HF/3-21G(*)	−318.739 693	0.0
		MP2/6-311+G**//HF/3-21G(*)	−320.828 319	
		MP3/6-311+G**//HF/3-21G(*)	−320.856 012	
		MP4/6-311+G**//HF/3-21G(*)	−320.878 717	
	π-complex	HF/3-21G(*)//HF/3-21G(*)	−318.751 718	−7.5
		MP2/6-311+G**//HF/3-21G(*)	−320.841 557	−8.3
		MP3/6-311+G**//HF/3-21G(*)	−320.869 104	−8.2
		MP4/6-311+G**//HF/3-21G(*)	−320.891 896	−8.3
	TS	HF/3-21G(*)//HF/3-21G(*)	−318.721 212	+11.6
		MP2/6-311+G**//HF/3-21G(*)	−320.817 409	+6.8
		MP3/6-311+G**//HF/3-21G(*)	−320.846 405	+6.0
		MP4/6-311+G**//HF/3-21G(*)	−320.871 074	+4.8
	product	HF/3-21G(*)//HF/3-21G(*)	−318.814 751	−47.1
		MP2/6-311+G**//HF/3-21G(*)	−320.900 689	−45.5
		MP3/6-311+G**//HF/3-21G(*)	−320.932 201	−47.8
		MP4/6-311+G**//HF/3-21G(*)	−320.951 521	−45.7
AlH_3 + propene	reactants	HF/3-21G(*)//HF/3-21G(*)	−358.767 724	0.0
		MP2/6-311+G**//HF/3-21G(*)	−361.261 910	
		MP3/6-311+G**//HF/3-21G(*)	−361.312 649	
		MP4/6-311+G**//HF/3-21G(*)	−361.338 858	
	π-complex	HF/3-21G(*)//HF/3-21G(*)	−358.785 235	−11.0
		MP2/6-311+G**//HF/3-21G(*)	−361.280 337	−11.6
		MP3/6-311+G**//HF/3-21G(*)	−361.330 396	−11.1
		MP4/6-311+G**//HF/3-21G(*)	−361.357 061	−11.4
	TS (favored)	HF/3-21G(*)//HF/3-21G(*)	−358.753 591	+8.9
		MP2/6-311+G**//HF/3-21G(*)	−361.259 779	+1.3
		MP3/6-311+G**//HF/3-21G(*)	−361.308 364	+2.7
		MP4/6-311+G**//HF/3-21G(*)	−361.337 185	+1.0
	TS (unfavored)	HF/3-21G(*)//HF/3-21G(*)	−358.744 643	+14.5
		HF/3-21G(*)//HF/3-21G(*)	−358.815 366	−29.9
		MP2/6-311+G**//HF/3-21G(*)	−361.312 100	−31.5
		MP3/6-311+G**//HF/3-21G(*)	−361.361 588	−30.7
		MP4/6-311+G**//HF/3-21G(*)	−361.386 617	−30.0
AlH_3 + propyne	reactants	HF/3-21G(*)//HF/3-21G(*)	−357.569 124	0.0
	π-complex	HF/3-21G(*)//HF/3-21G(*)	−357.584 642	−9.7
	TS (favored)	HF/3-21G(*)//HF/3-21G(*)	−357.552 430	+10.5
	TS (unfavored)	HF/3-21G(*)//HF/3-21G(*)	−357.546 795	+14.0
	product	HF/3-21G(*)//HF/3-21G(*)	−357.639 164	−43.9
$MeAlH_2 + C_2H_4$	reactants	HF/3-21G(*)//HF/3-21G(*)	−358.783 788	0.0
		MP2/6-311+G**//HF/3-21G(*)	−361.272 625	
		MP3/6-311+G**//HF/3-21G(*)	−361.324 013	
		MP4/6-311+G**//HF/3-21G(*)	−361.349 200	
	π-complex	HF/3-21G(*)//HF/3-21G(*)	−358.797 139	−8.4
	TS	HF/3-21G(*)//HF/3-21G(*)	−358.764 986	+11.7
		MP2/6-311+G**//HF/3-21G(*)	−361.267 369	+3.3
		MP3/6-311+G**//HF/3-21G(*)	−361.316 163	+4.9
		MP4/6-311+G**//HF/3-21G(*)	−361.343 902	+3.3
$MeAlH_2 + C_2H_2$	reactants	HF/3-21G(*)//HF/3-21G(*)	−357.578 756	0.0
	π-complex	HF/3-21G(*)//HF/3-21G(*)	−357.589 495	−6.7
	TS	HF/3-21G(*)//HF/3-21G(*)	−357.558 164	+12.9
AlH_3 + isobutene	reactants	HF/3-21G(*)//HF/3-21G(*)	−397.575 690	0.0
	π-complex	HF/3-21G(*)//HF/3-21G(*)	−397.606 252	−19.2
	TS	HF/3-21G(*)//HF/3-21G(*)	−397.578 406	+1.7
AlH_3 + 2-butyne	reactants	HF/3-21G(*)//HF/3-21G(*)	−396.397 388	0.0
	π-complex	HF/3-21G(*)//HF/3-21G(*)	−396.414 514	−10.7
	TS	HF/3-21G(*)//HF/3-21G(*)	−396.376 469	+13.1
AlH_3 + *cis*-2-butene	reactants	HF/3-21G(*)//HF/3-21G(*)	−397.586 624	0.0
	TS	HF/3-21G(*)//HF/3-21G(*)	−397.567 716	+11.9
$MeAlH_2$ + propene	reactants	HF/3-21G(*)//HF/3-21G(*)	−397.606 795	0.0
	TS	HF/3-21G(*)//HF/3-21G(*)	−397.589 557	+10.8
$Me_2AlH + C_2H_4$	reactants	HF/3-21G(*)//HF/3-21G(*)	−397.622 589	0.0
	TS	HF/3-21G(*)//HF/3-21G(*)	−397.600 722	+13.7

calculations may not add much to the discussion at hand. For example, the HF/3-21G(*) model predicts an activation energy of 10.0 kcal mol^{-1} for the reaction discussed in the preceding paragraph, much too high in comparison to either the experimental estimate or our post-Hartree–Fock calculated values. It is encouraging to note, however, that the predicted *trends* in activation energy do not vary dramatically with basis set or treatment of electron correlation. For example, methyl substitution at the α-carbon in ethylene is predicted at HF/3-21G(*) to lower the barrier by 1.1 kcal mol^{-1} relative to the unsubstituted case. MP4/6-311+G** predicts it to be 1.5 kcal mol^{-1} lower. We observe similar consistency between the relative predicted barriers for other cases, as well. We will therefore base some of our discussion of trends below on the HF/3-21G(*) results, bearing in mind that the absolute predictions are most likely too high.

Examining substituent effects on the prototypical reaction of AlH_3 with ethylene reveals several important trends in reactivity for these systems. Substitution of a methyl group at aluminum results in an increase of activation energy to 3.3 kcal mol^{-1} at the full MP4/6-311+G** level for $MeAlH_2$ + ethylene. Presumably the methyl group has the effect of stabilizing the $MeAlH_2$ fragment, requiring more energy to break the active Al–H bond during the insertion. Computed bond energies support this conjecture. The Al–H bond is calculated to be 0.9 kcal mol^{-1} stronger in $AlMeH_2$ than in AlH_3.[28] On the basis of our 3-21G(*) results, addition of a second methyl group at the aluminum would result in a 2 kcal mol^{-1} higher activation energy than with a single methyl group, and 3.7 kcal mol^{-1} higher than with no methyl substitution. Substitution of methyl at the β-C lowers the predicted activation energy. We attribute this to the electron-donating ability of the alkyl group, in this case stabilizing the positive charge developing on the β-C. In the parent AlH_3 + ethylene transition structure, the charge on the β-C is calculated to be +1.4e$^-$ (using CHELP II and the HF/3-21G(*) wavefunction) while in the AlH_3 + propene transition structure the corresponding value is +1.2e$^-$. The effect is even larger in the analogous reactions with alkynes.

For the reaction of AlH_3 with propene, the MP4(SDTQ)/6-311+G** calculation predicts a barrier of only 1.0 kcal mol^{-1}. With addition of two methyl groups at the β-C (AlH_3 + isobutylene reaction), we would expect an even greater stabilization of the transition state. The results concur. At the 3-21G(*) level, the activation energy is only 1.7 kcal mol^{-1}. Though we have not located a transition structure for this reaction using post-Hartree–Fock models, we would expect the barrier to be substantially lower than that predicted by 3-21G(*).

We can compare our results to Egger's estimation of the barrier to insertion of isobutylene into diisobutylaluminum hydride of 6 ± 3 kcal mol^{-1}.[3] Comparing this to the slightly lower (4.9 kcal mol^{-1}) barrier estimated by Egger for diethylaluminum hydride addition to ethylene suggests that bulky alkyl groups at the aluminum center may have a stronger influence on the barrier than stabilizing methyl groups at the β-C. However, the estimated energy differences are small, and within the error limits. Our results also show this trend. Comparing differences in activation energies between AlH_3 and $MeAlH_2$ with propene (1.9 kcal mol^{-1}) and between $MeAlH_2$ with propene and ethylene (0.9 kcal mol^{-1}) at 3-21G(*), we find a methyl group on the aluminum raises the barrier of the reaction by about 1.0 kcal mol^{-1} more than a methyl on the β-C lowers it.

We also considered the effects of substitution at the α-C and simultaneous substitution at both the α- and β-carbons. As suggested above, a methyl group at the α-C is energetically destabilizing in the transition structure and would, in turn, be expected to raise the activation energy. There is a 5.6 kcal mol^{-1} difference in activation energy at the 3-21G(*) level between the two orientations of AlH_3 with propene. With methyl groups at both carbons, as in *cis*-2-butene, the activation energy is 11.9 kcal mol^{-1} at 3-21G(*). This barrier is slightly higher than those for ethylene, or propene or even that for the addition of $MeAlH_2$ to ethylene. This is in agreement with the known preference for insertions at terminal olefin bonds with aluminum adding to the terminal carbon. The barrier toward the insertion of *cis*-2-butene into AlH_3 is also lower than the barrier for the Markovnikov addition of propene (by 2.6 kcal mol^{-1}), suggesting that at least for these simple systems the requirement for anti-Markovnikov addition is stricter than that for insertion into the terminal bond.

In summary we find the trends in reactivity for various substituted alkenes and alkylaluminum complexes at the 3-21G(*) level to be $H_2C{=}CR_2 \gg H_2C{=}CHR > H_2C{=}CH_2 > RCH{=}CHR$ and $MeAlH_2 > Me_2AlH_2$. The corresponding trends for the reactivity of substituted alkynes at the 3-21G(*) level are $HC{\equiv}CR > HC{\equiv}CH > RC{\equiv}CR$. Experimentally, Eisch[4] determined the trends in reactivity to be $HC{\equiv}CR > RC{\equiv}CR > H_2C{=}CHR > RCH{=}CHR$. Eisch indicates that alkynes are more reactive than alkenes and suggests that a decrease in the F strain[29] is the root cause. Internal multiple bonds are less reactive, again presumably due to an increase in steric interactions between the substituents on the organic fragment with the ligands on the aluminum. Our results at all theoretical levels agree with the substituent effects found experimentally with one exception: we find the alkenes to be more reactive (i.e. to have lower barriers) than alkynes. However, since the activation energies themselves are of such a small magnitude, corrections to the barriers for zero-point energies of vibration and to temperatures greater than 0 K could be significant.

In Table VI, selected HF/3-21G(*) energies have been corrected to higher temperatures (298 and 445 K) and for the zero-point energies of vibration. While the latter corrections do not affect the differences in activation energies significantly, inclusion of temperature corrections has a greater impact. The corrections generally affected the alkene barriers more than the alkyne barriers due to the larger number of frequency terms in the alkene corrections. At 298 K the activation energy difference between addition of ethylene and acetylene to AlH_3 is only 0.1 kcal mol^{-1} and is only 0.5 kcal mol^{-1} between the addition of propene and propyne to the same substrate. In comparison, the difference at 0 K is 1.6 kcal mol^{-1} in both cases.

At 445 K, a temperature comparable to that used in the experimental work on these systems, we find a complete reverse in the predicted relative reactivity of alkenes and alkynes. At this higher temperature, the corrections

(28) Bundens, J. W., unpublished calculations at the MP2/6-31G**//HF/3-21G(*) level.

(29) Brown, H. C.; Davidson, N. *J. Am. Chem. Soc.* **1942**, *64*, 316. Buhr, G.; Muller, G. E. *Chem. Ber.* **1955**, *88*, 251.

Table VI. Corrections for Zero-Point Vibrational Energy and to Higher Temperatures[a] made to Selected Structures at the HF/3-21G(*) Basis

reaction	structure	correction (kcal/mol) 298 K	correction (kcal/mol) 445 K	$\Delta E_{corrected}$[b] (kcal/mol) 298 K	$\Delta E_{corrected}$[b] (kcal/mol) 445 K
$AlH_3 + C_2H_4$	reactants	48.4	56.0	0.0	0.0
	π-complex	49.3	61.7	-8.8	-4.0
	TS	49.7	64.4	+11.3	+18.4
	product	52.1		+39.6	
$AlH_3 + C_2H_2$	reactants	34.0	40.3	0.0	0.0
	π-complex	34.6	44.9	-6.9	-2.9
	TS	33.8	44.0	+11.4	+15.2
	product	39.1		+53.4	
AlH_3 + propene	reactants	67.1	80.2	0.0	0.0
	π-complex	69.0	89.8	-8.9	-1.2
	TS	70.3	93.8	+12.0	+22.5
AlH_3 + propyne	reactants	51.7	60.9	0.0	0.0
	π-complex	52.9	68.0	-8.5	-2.6
	TS	53.7	71.1	+12.5	+20.7

[a] See ref 19 in text. [b] $\Delta E_{corrected}$ refers to the corrected binding energy for π-complexes, E_a forward for TS and E_a* backward for products (see Figure 6).

increase the activation energy of the reaction with ethylene by 8.4 kcal mol^{-1} while the barrier to the addition of acetylene is only 3.6 kcal mol^{-1} higher than at 0 K. The difference in activation energies for the additions of ethylene and acetylene to AlH_3 increases to 4.8 kcal mol^{-1}, and is now in the correct direction.

At both 298 and 445 K we find ethylene and acetylene to be significantly more reactive than their corresponding β-methyl-substituted derivatives. At the higher temperature there is a 5.2 kcal mol^{-1} decrease in the barrier for the addition of AlH_3 to ethylene compared to that for propene and a 6.6 kcal mol^{-1} decrease in barrier between the analogous reactions with acetylene and propyne. On the basis of the experimental trends which suggest that increasing substitution increases reactivity, this is not expected; however, experimental data for the unsubstituted systems is not available. In retrospect, this is not surprising to us, in that more vibrational modes are available to the more highly substituted methyl derivatives and hence we would expect more energy to be in "useful" modes in the parent compounds. Since the parents are also much less sterically demanding than even the singly substituted derivatives, this may be sufficient to account for their unanticipated reactivity relative to the substituted systems.

Back Reaction. There are many experimental analyses of β-hydride elimination reactions both in the gas phase and on aluminum surfaces. The range of activation energies for these endothermic reactions with trialkylaluminum compounds is found to be approximately 24–37 kcal mol^{-1} both in the gas phase and on the aluminum surface.[30] For example, Smith and Wartik found the activation energy for the elimination of ethylene from triethylaluminum to be 30 kcal/mol[31] and Egger found it to be 26.6 kcal mol^{-1} for isobutylene from Al(*i*-Bu)$_3$.[3] On the aluminum surface, Bent et al. also report a barrier of approximately 30 kcal mol^{-1} for the elimination of isobutylene.[30a] Bent speculates that the mechanism describing the reaction of organometallic aluminum compounds may also be an appropriate description of the growth reaction occurring on an aluminum surface.[30b]

The predicted MP4(SDTQ)/6-311+G**//HF/3-21G(*) value for the barrier to the elimination of ethylene from $H_2AlC_2H_5$ is 39.6 kcal mol^{-1}. Corrections to 298 K and for zero-point vibrational energy do not affect the predicted trends in activation energy. Previous theoretical calculations on this reverse of the hydroalumination reaction with alane and ethylene at different levels of theory fall close to the experimental range as well. Higashi et al.[9] report a barrier of approximately 32 kcal mol^{-1} while it is estimated by Gropen and Haaland to be 41 kcal mol^{-1}.[6]

Conclusions

(1) Calculated activation energies for both forward and backward reactions compare favorably with experimental information when corrected for zero-point energies of vibration and to experimental temperatures.

(2) Intrinsically (i.e. at 0 K) alkenes were found to be more reactive than alkynes. Raising the temperature to 445 K and adding zero-point energy corrections resulted in alkynes being more reactive than alkenes, in agreement with experimentally observed trends.

(3) Hydroalumination reactions favor insertions at terminal C–C bonds with aluminum adding to the terminal carbon. Substitution of a methyl group at the α-C increased the activation energy for both alkenes and alkynes.

(4) Substitution of a methyl group at the β-C of the alkene or alkyne stabilized the transition structure via electron donation to the β-C thereby enhancing reactivity for both the forward and backward reactions.

We are currently exploring a similar mechanism for carboalumination. Recently, we have located the transition structure for the insertion of ethylene into the Al–C bond of H_2AlCH_3. Work is in progress to characterize this and related structures.

Acknowledgment. The support of Bryn Mawr College's Academic Computing Center and a grant from the National Center for Supercomputing Applications for time on their Cray-YMP/4 are gratefully acknowledged. M.M.F. thanks Dr. Nicolaas Hommes for helpful conversations. J.W.B. wishes to thank Professor Frank Mallory for helpful discussions and GAANN for fellowship support.

Supplementary Material Available: Tables of Cartesian coordinates for optimized transition structures, intermediates, and products (10 pages). Ordering information is given on any current masthead page.

OM920667X

(30) (a) Bent, B. E.; Nuzzo, R. G.; Dubois, L. H. *J. Am. Chem. Soc.* **1989**, *111*, 1634. (b) Bent, B. E.; Nuzzo, R. G.; Zegarski, B. R.; Dubois, L. H. *J. Am. Chem. Soc.* **1991**, *113*, 1137. (c) Egger, K. W.; Cocks, A. T. *Trans. Faraday Soc.* **1971**, *67*, 2629.

(31) Smith, W. L.; Wartik, T. *J. Inorg. Nucl. Chem.* **1967**, *29*, 629.